Transactions of the 15th International Conference on
Structural Mechanics in Reactor Technology (SMiRT-15)
Seoul, Korea, August 15-20, 1999

Ultimate Strength Analysis of Stiffened Shell Structures

Sung Pil Chang[1], Myeong Su Choi[1] and Moon Young Kim[2]

1) Seoul National University, Korea
2) Sung Kyun Kwan University, Korea

ABSTRACT

For the ultimate strength analysis of stiffened plate and shell structures, total Lagrangian formulation is presented based upon the degenerated shell element. Assumed strain concept is adopted in order to overcome shear locking phenomena and to eliminate spurious zero energy mode. In the calculation of the stiffness matrix, the element formulation takes into account the effect of finite rotation increments by retaining second order rotation terms in the incremental displacement field. In the elasto-plastic analysis the return mapping algorithm, based on the consistent elasto-plastic tangent modulus, is applied to anisotropic shell structure.

1. INTRODUCTION

A degenerate shell element which is easily applicable to plate and shell analysis was first presented by Ahmad, Irons and Zienkiewicz[1]. This element was derived from a three dimensional element by applying a so-called degeneration process. The classical Krichhoff hypothesis was no longer fulfilled since both in-plane and shear strains were taken into account. This element and its numerous versions have been used for both linear and nonlinear problems. However, these elements suffer from shear locking and membrane locking.

To overcome these phenomena, a number of authors have developed elements based on the "assumed strain" concept. MacNeal[2] used an assumed strain concept to develop a 4-node element and 6-node triangular element. Huang and Hinton[3,4] have proposed elements based on the use of assumed (non-physical) covariant transverse shear strains referred to element natural coordinate systems, for membrane strains used a local Cartesian coordinate system to separate bending and membrane strains and mixed interpolated only the membrane part. Bucalem and Bathe[5,6] presented the elements based on the mixed interpolation of tensorial components approach for 9-node and 16-node shell element.

In the development of structural elements for the post-buckling analysis, the consideration of large rotations introduces additional difficulties due to the non-vectorial nature of finite rotations. In the conventional non-linear formulation[7] for degenerate shell elements, the tangent stiffness matrix is derived by assuming infinitesimal rotation increments (rotation increments linearization) and the effect of large rotation increments is considered only during the equilibrium iterations when calculating the stresses. The

kinematics of large rotation was studied extensively by Argyris[8] and formulations that take into account the effect of finite rotation increments on the resulting stiffness have been presented by Surana[9].

In this study, the element formulations are based on the degenerate shell element and the assumed strain concept is adopted. In the elasto-plastic analysis the return mapping algorithm is applied. A finite element formulation accounting the second order effects of finite rotations is presented in order to analyze the post-buckling and elasto-plastic behaviors of stiffened plate and shell structures.

2. FORMULATION OF SHELL ELEMENT CONSIDERING LARGE ROTATIONS

2.1 Effect of Finite Rotations

The position vector of any point inside the shell element at time t can be expressed as,

$$ {}^{t}X_i = \sum_{k=1}^{n} N_k \, {}^{t}X_i^k + \frac{t}{2} \sum_{k=1}^{n} N_k h_k \, {}^{t}V_{3i}^k \tag{1} $$

The incremental displacement from the configuration at time t to the configuration at time $t+\Delta t$ is defined as,

$$ \overline{U}_i = {}^{t+\Delta t}X_i - {}^{t}X_i = \sum_{k=1}^{n} N_k U_i^k + \frac{t}{2} \sum_{k=1}^{n} N_k h_k \left({}^{t+\Delta t}V_{3i}^k - {}^{t}V_{3i}^k \right) \tag{2} $$

From Argyris's studies[8], the changes in the direction cosines of the normal can be expressed as

$$ {}^{t+\Delta t}\mathbf{V}_3^k - {}^{t}\mathbf{V}_3^k = -{}^{t}\mathbf{V}_2^k \theta_1^k + {}^{t}\mathbf{V}_1^k \theta_2^k - \tfrac{1}{2} {}^{t}\mathbf{V}_3^k \left(\theta_1^{k2} + \theta_2^{k2} \right) \tag{3} $$

By substituting Eq. (3) into (2), the resulting incremental displacement of any point inside the shell element can be expressed by two terms,

$$ \overline{U}_i = U_i + U_i^* \tag{4} $$

where U_i is the incremental displacement obtained considering only infinitesimal rotation increments (standard linearization), and U_i^* is the extra term due to the quadratic terms in the incremental displacement.

Hence,

$$ U_i = \sum_{k=1}^{n} N_k U_i^k + \frac{t}{2} \sum_{k=1}^{n} N_k h_k \left(-{}^{t}V_{2i}^k \theta_1^k + {}^{t}V_{1i}^k \theta_2^k \right) \tag{5} $$

and

$$ U_i^* = \frac{t}{2} \sum_{k=1}^{n} N_k \frac{h_k}{2} \left[-{}^{t}V_{3i}^k \left(\theta_1^{k2} + \theta_2^{k2} \right) \right] \tag{6} $$

In the usual formulation, the linear and nonlinear strain-displacement transformation matrices used in the total Lagrangian formulation may be obtained from Eq. (1) to Eq. (6), except for the second order terms. However for more accurate evaluation of the element geometric stiffness of structural elements, the second order terms with respect to the generalized rotational degree of freedom should be added to the nonlinear strain terms of the incremental equations.

2.2 Incremental Equilibrium Equations

Virtual work principle for the general continuum is expressed as[7],

$$ \int_V {}^{t+\Delta t}_{0}S_{ij} \cdot \delta \left({}^{t+\Delta t}_{0}\varepsilon_{ij} \right) {}^{0}dV = {}^{t+\Delta t}R = \int_S {}^{t+\Delta t}T_i \delta \, {}^{t+\Delta t}U_i \, {}^{0}dS \tag{7} $$

where

$$ {}^{t+\Delta t}_{0}\varepsilon_{ij} = \frac{1}{2}\left({}^{t+\Delta t}_{0}U_{i,j} + {}^{t+\Delta t}_{0}U_{j,i} + {}^{t+\Delta t}_{0}U_{k,i}\,{}^{t+\Delta t}_{0}U_{k,j}\right) \tag{8} $$

In these formulae, ${}^{t+\Delta t}_{0}S_{ij}$ and ${}^{t+\Delta t}_{0}\varepsilon_{ij}$ are the second Piola-Kirchhoff stress and the Green-Lagrange strain at time $t+\Delta t$ referred to the configuration at time 0, respectively. The incremental displacement components at time t and $t+\Delta t$ are

$$ {}^{t+\Delta t}U_i = {}^{t}U_i + U_i + U_i^* \tag{9} $$

where U_i denotes the first order terms of the displacement parameters and U_i^* denotes the second order terms due to large rotations, and their sum consists of incremental displacement. Substituting Eq. (9) into Eq. (8) and neglecting higher order terms, the incremental equation of strains is expressed as

$$ {}_0\varepsilon_{ij} = {}^{t+\Delta t}_{0}\varepsilon_{ij} - {}^{t}_{0}\varepsilon_{ij} = {}_0e_{ij} + {}_0\eta_{ij} + {}_0e^*_{ij} \tag{10} $$

where

$$ \begin{aligned} {}_0e_{ij} &= \frac{1}{2}\left({}_0U_{i,j} + {}_0U_{j,i} + {}^{t}_{0}U_{k,i}\,{}_0U_{k,j} + {}_0U_{k,i}\,{}^{t}_{0}U_{k,j}\right) \\ {}_0\eta_{ij} &= \frac{1}{2}\,{}_0U_{k,i}\,{}_0U_{k,j} \\ {}_0e^*_{ij} &= \frac{1}{2}\left({}_0U^*_{i,j} + {}_0U^*_{j,i} + {}^{t}_{0}U_{k,i}\,{}_0U^*_{k,j} + {}_0U^*_{k,i}\,{}^{t}_{0}U_{k,j}\right) \end{aligned} \tag{11} $$

The ${}_0e_{ij}$ and ${}_0\eta_{ij}$ are the conventional linear and non-linear Green-Lagrange strain increment respectively, and ${}_0e^*_{ij}$ is the linear strain increment due to U_i^*.

The incremental equations of equilibrium for a general continuum in the total Lagrangian formulation is expressed as

$$ \int_V \left({}_0C_{ijkl}\,{}_0e_{kl}\delta e_{ij} + {}^{t}_{0}S_{ij}\delta\,{}_0\eta_{ij} + {}^{t}_{0}S_{ij}\delta e^*_{ij}\right){}^{0}dV = {}^{t+\Delta t}R - \int_V {}^{t}_{0}S_{ij}\delta\,{}_0e_{ij}\,{}^{0}dV \tag{12} $$

where, the first term gives the element elastic stiffness and the last term the element nodal force, whereas the geometric stiffness results from the contribution of non-linear strains, i.e. the second and third terms.

2.3 Assumed Strain Finite Element

According to Mindlin-type theories, the rotations are independent of the displacements in both plates and shells. When the finite element method is used in conjunction with Mindlin-type formulations, the shear strain energy predicted by the finite element analysis can be magnified unreasonably even though the average value of the shear strains over the area tends to zero. An artificial method for the elimination of shear and membrane locking is to interpolate new strain fields, so called 'assumed strain field', from the strain values at the sampling points which are appropriately located in individual elements. A number of authors have developed elements based on the "assumed strain" concept. Among these studies, Huang and Hinton[3] have proposed elements based on the use of assumed covariant transverse shear strains referred to element natural coordinate systems, for membrane strains used a local Cartesian coordinate system to separate bending and membrane strains and mixed interpolated only the membrane part, consequently two distinct coordinate systems are required and some complicated routine is produced. Bucalem and Bathe[6] presented the elements based on the mixed interpolation of tensorial components(covariant strain terms) approach for 9-node and 16-node shell element.

In this study, assumed covariant strain field is used to define new strain field and interpolated these strain values to the nine Gauss points from the six sampling points(Fig. 1.). After interpolation, all strain terms are transformed to local coordinate system to calculate physical strains, the membrane strains are extracted from bending strains after transformation. The stiffness matrix terms, associated with shear and membrane strains, are replaced new strain terms.

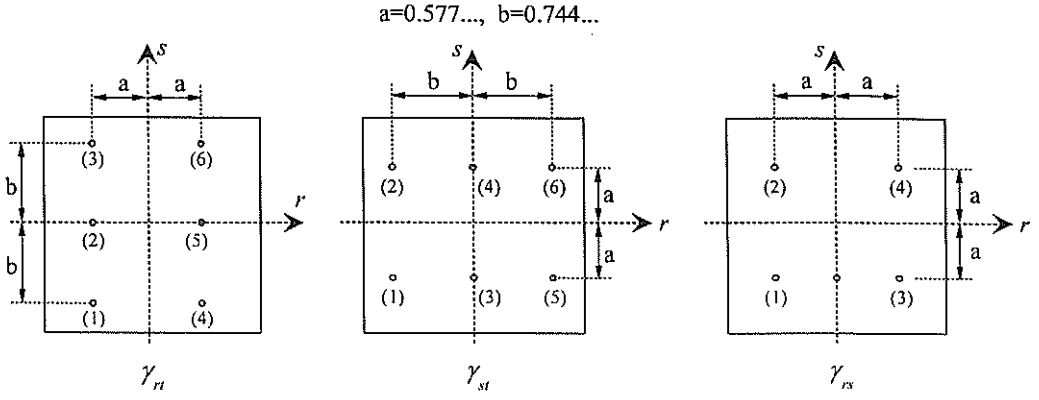

Fig. 1. Sampling Points for the 9-node Lagrangian Element

2.4 Modeling of Stiffener Element

In the general shell element, five degrees of freedom are specified at each nodal point. Whereas in the stiffened plate and shell element or in the thin-walled structures where the elements are connected with finite angle, six degrees of freedom are required at the connection nodes.

In this study, all nodal points have five degree of freedom except the connection points connecting the main elements and stiffener elements. In the connection nodes, the rotational degrees of freedom of the stiffener element are referred to that of main shell elements. Therefore coordinate transformation is required only for the stiffener element, and no transformation is needed for the main shell element.

3. ELASTO-PLASTIC ANALYSIS OF SHELL

3.1 Stress-Strain Relations

In this study the elastic constitutive relation for anisotropic material[10] is used with an assumption that the reference system of orthogonal axes is parallel to the principal material axis. The generalized Von-Mises yield criterion is employed to consider the anisotropic materials. The consistent elasto-plastic tangent moduli[1] is applied to anisotropic shell element, to define the relationship between the incremental stress and strain.

The basic equations in elasto-plastic problems may be summarized as follows

1) incremental strain : $d\boldsymbol{\varepsilon} = d\boldsymbol{\varepsilon}^e + d\boldsymbol{\varepsilon}^p$

2) elastic stress-strain relation : $\boldsymbol{\sigma} = \mathbf{D}\boldsymbol{\varepsilon}^e$

3) flow rule : $d\boldsymbol{\varepsilon}^p = d\lambda \mathbf{A}\boldsymbol{\sigma}$

4) yield function : $\Psi = \frac{1}{2}\boldsymbol{\sigma}^T \mathbf{A}\boldsymbol{\sigma} - \frac{1}{3}\sigma_Y^2\left(\bar{e}^p\right) = 0$

where, $\mathbf{A}$ and $\mathbf{D}$ are the anisotropic parameter and elasticity matrix for anisotropic materials[10], respectively.

The plastic strains ${}^{t+\Delta t}\boldsymbol{\varepsilon}^p$ and ${}^{t+\Delta t}\bar{e}^p$ are determined by integration of the flow rule and hardening law over the time step from t to $t+\Delta t$. If the 'generalized midpoint rule' is used to integrate the flow rule, the plastic strains at time $t+\Delta t$ can be expressed as

$$ {}^{t+\Delta t}\varepsilon^{p} = {}^{t}\varepsilon^{p} + \int^{t+\Delta t} d\lambda \mathbf{A}\sigma dt = {}^{t}\varepsilon^{p} + d\lambda \mathbf{A}^{t+\alpha\Delta t}\sigma \tag{13} $$

$$ {}^{t+\Delta t}\bar{e}^{p} = {}^{t}\bar{e}^{p} + \int^{t+\Delta t} d\lambda\sqrt{\tfrac{2}{3}}\bar{\phi}dt = {}^{t}\bar{e}^{p} + d\lambda\sqrt{\tfrac{2}{3}}{}^{t+\alpha\Delta t}\bar{\phi} \tag{14} $$

where $0 < \alpha \le 1$, ${}^{t+\alpha\Delta t}\sigma$ and ${}^{t+\alpha\Delta t}\bar{\phi}$ are defined as follows.

$$ {}^{t+\alpha\Delta t}\varepsilon = \alpha^{t+\Delta t}\varepsilon + (1-\alpha)^{t}\varepsilon = {}^{t}\varepsilon + \alpha\nabla^{S}U \tag{15} $$

$$ {}^{t+\alpha\Delta t}\varepsilon^{p} = \alpha^{t+\Delta t}\varepsilon^{p} + (1-\alpha)^{t}\varepsilon^{p} \tag{16} $$

$$ {}^{t+\alpha\Delta t}\bar{e}^{p} = \alpha^{t+\Delta t}\bar{e}^{p} + (1-\alpha)^{t}\bar{e}^{p} \tag{17} $$

$$ {}^{t+\alpha\Delta t}\sigma = \mathbf{D}\left[{}^{t+\alpha\Delta t}\varepsilon - {}^{t+\alpha\Delta t}\varepsilon^{p}\right] \tag{18} $$

$$ {}^{t+\alpha\Delta t}\bar{\phi} = \left[{}^{t+\alpha\Delta t}\sigma^{T}\mathbf{A}^{t+\alpha\Delta t}\sigma\right]^{1/2} \tag{19} $$

Making use of Eqs. (13)-(19), and after some manipulation, the incremental stress strain relationship can be obtained as

$$ {}^{t+\alpha\Delta t}d\sigma = \left[\Xi - \frac{\Xi\mathbf{A}^{t+\alpha\Delta t}\sigma \cdot {}^{t+\alpha\Delta t}\sigma^{T}\mathbf{A}\Xi}{{}^{t+\alpha\Delta t}\sigma^{T}\mathbf{A}\Xi\mathbf{A}^{t+\alpha\Delta t}\sigma(1+\beta)}\right]{}^{t+\alpha\Delta t}d\varepsilon \tag{20} $$

or

$$ {}^{t+\alpha\Delta t}d\sigma = \Xi_{ep}\,{}^{t+\alpha\Delta t}d\varepsilon \tag{21} $$

where Ξ_{ep} is called the 'consistent elasto-plastic tangent muduli', and

$$ \gamma_2 = 1 - \tfrac{2}{3}\alpha\sigma_Y' d\lambda\,; \quad \beta = \frac{2}{3}\frac{\sigma_Y'}{\gamma_2}\frac{{}^{t+\alpha\Delta t}\sigma^{T}\mathbf{A}^{t+\alpha\Delta t}\sigma}{{}^{t+\alpha\Delta t}\sigma^{T}\mathbf{A}\Xi\mathbf{A}^{t+\alpha\Delta t}\sigma} \tag{22} $$

In the limiting case of $\Delta t \to 0$ or $\alpha \to 0$, it follows that $\gamma_2 \to 1$ and $\Xi \to \mathbf{D}$. Therefore Ξ_{ep} can be expressed as

$$ \Xi_{ep} = \mathbf{D} - \frac{\mathbf{DA}\sigma \cdot \sigma^{\mathrm{T}}\mathbf{AD}}{\sigma^{\mathrm{T}}\mathbf{ADA}\sigma + \sigma_Y'\sigma^{\mathrm{T}}\mathbf{A}\sigma} = \mathbf{D} - \frac{\mathbf{Da}\cdot\mathbf{a}^{T}\mathbf{D}}{\mathbf{a}^{T}\mathbf{Da} + \sigma_Y'} \tag{23} $$

which coincide with the classical elasto-plastic tangent muduli, $\mathbf{D}_{ep}$ [10].

3.2 Update Algorithm

In the general material nonlinear analysis by Newton-Raphson iteration method, the iteration process can be divided into two parts. First is calculating the trial stress using linearized tangential stiffness which corresponds to the elastic predictor. Second is calculating exact stress state with the appropriate yield condition which corresponds to the plastic corrector. In the elastic predictor phase, the quadratic convergence rate can be obtained by using the consistent elasto-plastic tangent modulus Eq. (21) rather than classical elasto-plastic tangent modulus Eq. (23). Furthermore, the accuracy of the solution can be obtained by using the return mapping algorithm in the plastic corrector phase. The second part of the algorithm defines a relaxation process towards the yield surface often referred as return mapping[11].

4. NUMERICAL EXAMPLES

4.1 Clamped Quadratic Shell

In this example the elasto-plastic analysis of a clamped quadratic shell, under a central point load, is performed. The following material properties are considered

Isotropic material properties :

$$E_x = E_y = 3.0\times10^4 \quad G = 11540.0 \quad \nu = 0.3$$

$$\sigma_{0x} = \sigma_{0y} = \sigma_{045} = 30.0 \quad \tau_{012} = \tau_{013} = \tau_{023} = 17.32 \quad H' = 300.0$$

Anisotropic material properties :

$$\sigma_{0y} = 40.0 \quad \sigma_{045} = 35.0 \quad \tau_{012} = 20.2$$

the remaining values are the same for the isotropic case (units : MN, m)

The shell geometry is defined in Fig. 2., where the thickness is taken as $h = 0.2$ and the span length as $L = 6.0$. Fig. 2. also shows the load-central deflection relationship using six layers through the shell thickness, where (H) denotes the Huang's results[12] and (R) denotes the results of the present study using return mapping algorithm. As shown in Table 1., the iteration numbers to get the solution are considerably decreased by using the return mapping algorithm.

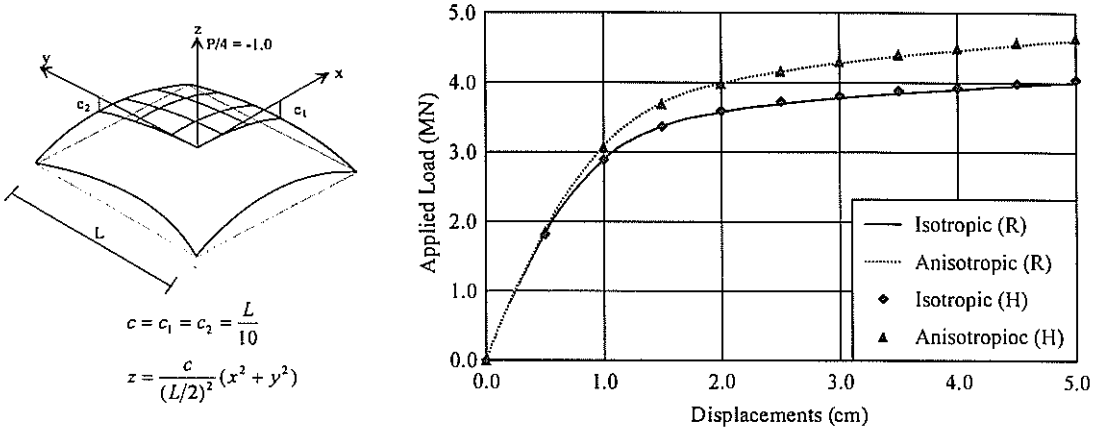

Fig. 2. Clamped Quadratic Shell under a Central Point Load

Table 1. Comparison of Iteration Numbers for Clamped Quadratic Shell

Load Step	Classical Method		Consistent Method	
	Isotropic	Anisotropic	Isotropic	Anisotropic
1	3	3	2	2
2	3	3	3	3
3	3	3	3	3
4	4	3	2	2
5	4	5	2	2
6	5	4	2	2
7	4	5	2	2
8	5	4	2	2
9	5	4	2	2
10	4	4	2	2
Total	40	38	22	22

4.2 Elastic and Elasto-Plastic Behavior of Curved Cantilever

Buckling and post-buckling analysis of a curved cantilever is performed considering the elastic and elasto-plastic material properties. Fig. 3. shows the finite element mesh and the material properties, where the top and bottom flanges are modeled as stiffener element since the flanges are connected to the web with finite angle (90 degree). Fig. 4. shows the load-displacement curves for negative and positive end forces. As shown in Fig. 4., in case of negative end force the lateral buckling and plastic failure is occurred at the same time around the linear buckling load, but in case of positive end force the plastic failure is occurred below the lateral buckling load. The linear buckling loads for negative and positive end loads are 17.59 kN and 460.85 kN, respectively.

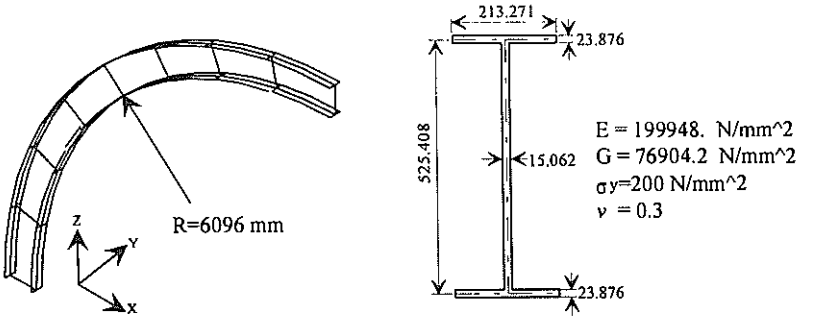

(a) Modeling (b) Cross section and material properties

Fig. 3. Curved Cantilever with I-type Cross Section

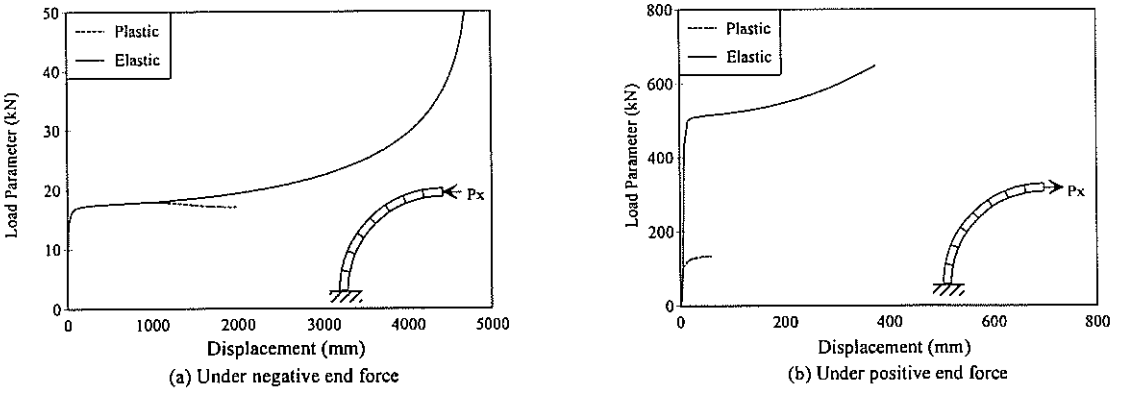

(a) Under negative end force (b) Under positive end force

Fig. 4. Load-Displacement Curves for Curved Cantilever

5. CONCLUSION

In this study the ultimate strength analysis, including the buckling, post-buckling, elasto-plastic analysis, of stiffened shell structures is preformed using the degenerate shell element. The assumed strain concept is adopted to overcome locking phenomena, which is the main defect of the displacement based isoparametric finite element especially for thin shell situation, and to eliminate the spurious zero energy modes occurring when reduced or

selective integration methods are used. In the buckling and post-buckling analysis, more exact solutions are obtained by evaluating the total Green-Lagrangian strains corresponding to total displacements and by including the effect of second order rotation terms in the incremental displacement field. In the elasto-plastic analysis, the return mapping algorithm is applied to the anisotropic shell structures. Unlike the classical formulations for elasto-plastic analysis, the consistent elasto-plastic tangent modulus is obtained by using the generalized midpoint rule to integrate the flow rule.

ACKNOWLEDGEMENTS

The authors are grateful for the support provided by a grant from the Korea Science & Engineering Foundation(KOSEF) and Safety and Structural Integrity Research Center at the Sungkyunkwan University.

REFERENCES

1. S. Ahmad, B. M. Irons, and O. C. Zienkiewicz, "Analysis of thick and thin shell structures by curved element", *International Journal for Numerical Methods in Engineering*, Vol. 2, 1970, pp. 419-451.
2. R. H. Macneal, "Derivation of element stiffness matrices by assumed strain distributions", *Nuclear Engineering Des.* Vol. 70, 1982, pp. 2-12.
3. H. C. Huang and E. Hinton, "A New Nine Node Degenerated Shell Element with Enhanced Membrane and Shear Interpolation", *International Journal for Numerical Methods in Engineering*, Vol. 22, pp.73-92, 1986.
4. H. C. Huang, "Implementation of assumed strain degenerated shell elements", *Computers and Structures*, Vol. 25, 147-155, 1987.
5. K. J. Bathe and E. N. Dvorikin, "A four-node plate bending element based on Mindlin/Reissner plate theory and a mixed interpolation", *International Journal for Numerical Methods in Engineering*, Vol. 21, 1985, pp. 367-383.
6. M. L. Bucalem and K. J. Bathe, "Higher-Order MITC General Shell Elements", *International Journal for Numerical Methods in Engineering*, V.36, pp.3729-3754, 1993.
7. K. J. Bathe, *Finite Element Procedures in Engineering Analysis*, Prentice-Hall, 1996.
8. J. Argyris, "An excursion into large rotations", *Computer Methods in Applied Mechanics and Engineering*, Vol. 32, 1982, pp. 85-155.
9. K. S. Surana, "Geometrically non-linear formulation for the curved shell elements", *International Journal for Numerical Methods in Engineering*, Vol. 19, 1983, pp. 581-615.
10. E. Hinton and D. R. J. Owen, *Finite Element Software for Plates and Shells*, Pineridge Press, 1985.
11. J. C. SIMO and R. L. TAYLOR, "A Return Mapping Algorithm for Plane Stress Elastoplasticity", *International Journal for Numerical Methods in Engineering*, Vol. 22, pp. 649-670, 1986.
12. H. C. Huang, *Static and Dynamic Analyses of Plates and Shells*, Springer-Verlag, Berlin, 1989.